

# Rational Design of Preintercalated Electrodes for Rechargeable Batteries

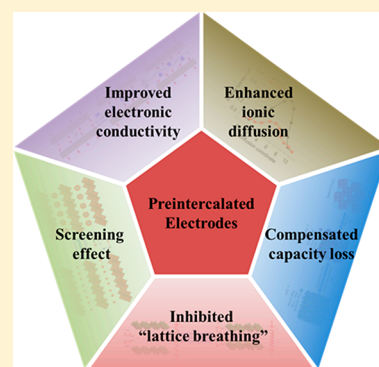
Xuhui Yao,<sup>†,‡,§</sup> Yunlong Zhao,<sup>\*,‡,§</sup> Fernando A. Castro,<sup>‡,§</sup> and Liqiang Mai<sup>\*,†,‡</sup>

<sup>†</sup>State Key Laboratory of Advanced Technology for Materials Synthesis and Processing, Wuhan University of Technology, Wuhan 430070, People's Republic of China

<sup>‡</sup>Advanced Technology Institute, University of Surrey, Guildford, Surrey GU2 7XH, United Kingdom

<sup>§</sup>National Physical Laboratory, Teddington, Middlesex TW110LW, United Kingdom

**ABSTRACT:** Rational design of the morphology and complementary compounding of electrode materials have contributed substantially to improving battery performance, yet the capabilities of conventional electrode materials have remained limited in some key parameters including energy and power density, cycling stability, etc. because of their intrinsic properties, especially the restricted thermodynamics of reactions and the inherent slow diffusion dynamics induced by the crystal structures. In contrast, preintercalation of ions or molecules into the crystal structure with/without further lattice reconstruction could provide fundamental optimizations to overcome these intrinsic limitations. In this Perspective, we discuss the essential optimization mechanisms of preintercalation in improving electronic conductivity and ionic diffusion, inhibiting “lattice breathing” and screening the carrier charge. We also summarize the current challenges in preintercalation and offer insights on future opportunities for the rational design of preintercalation electrodes in next-generation rechargeable batteries.



Given the excessive consumption of fossil energy and the looming concerns of the climate problem, renewable energy resources such as solar, wind, and tide have entered the public spotlight, stimulating research of high-efficiency energy storage systems.<sup>1,2</sup> Among the studies so far, the rechargeable prototype of a “rock-chair battery” is still considered as one of the most promising candidates for energy storage in the applications of portable devices, electric vehicles, and grid-scale stations.<sup>3,4</sup> It functions as a conversion device between chemical energy and electrical energy by shuttling ions between the cathode and the anode.<sup>5</sup> Since the successful LiCoO<sub>2</sub> and LiFePO<sub>4</sub> electrodes were introduced by Goodenough et al. and have been commercialized for a long time, much effort has been focused on further optimization of batteries, including development of novel high-performance electrode materials, rational design of the morphologies and complementary compounding of electrode materials that can further improve the energy and power density, and the cycling stability.<sup>6–8</sup> Despite advancements over the past decades, substantial limitations of electrode materials have remained due to their intrinsic properties, especially the restricted thermodynamics of reactions and the inherent slow diffusion dynamics induced by the crystal structures. Taking the beyond-Li-ion battery for instance, their electrodes seriously suffer from the above restrictions due to the limited diffusion channels and crystal degradation associated with larger ions (e.g., Na<sup>+</sup> and K<sup>+</sup>) or multivalent ions (e.g., Mg<sup>2+</sup> and Zn<sup>2+</sup>) intercalation/deintercalation.<sup>9–11</sup> Recognizing this issue, scientists have

strived to develop strategies that can realize fundamental crystal optimizations, such as via preintercalating of ions or molecules into the crystal structure with/without further lattice reconstruction.

Preintercalation strategies provide fundamental and issues-oriented optimizations for battery electrode materials, breaking the limitations of intrinsic crystallographic structures.

Preintercalation has received a lot of attention as an effective approach to improve electrode performance in recent years.<sup>12,13</sup> The key feature of this approach is that small fractions of the electrochemically inactive or partially active elements/guests are inserted into the host structure before battery cycling. These intercalated guest species, including organic or inorganic ions, organic molecules, functional groups and water, interact with the adjacent host atoms and the ion carriers through bonding, repulsion, or coordination, optimizing the inherent structure of hosts and the transport property of ion carriers significantly. The potentially revolutionary advantage of such an optimization

Received: December 31, 2018

Accepted: February 18, 2019

Published: February 18, 2019

process has led to huge interest in the research of preintercalation (Figure 1). Generally, there are two different

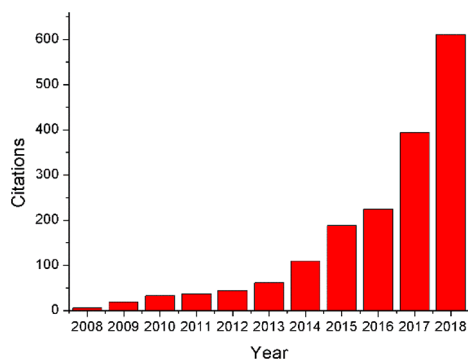


**Figure 1.** Number of citations on preintercalation published between 2008 and 2018. Data was collected from Web of Science by searching the keywords “pre-intercalation” and “pre-intercalated” and excluding the irrelevant paper.

approaches that have been developed to achieve preintercalated materials: chemical preintercalation and electrochemical preintercalation. In chemical preintercalation, guest species are usually inserted during the initial material synthesis through chemical reactions via solvothermal method, microwave hydrothermal method, etc. or with further chemical treatments. In electrochemical preintercalation, guest species are usually inserted into the target materials through electrochemical strategies such as galvanotactic charge/discharge or during initial synthesis such as via electrodeposition reactions. Given the different reactions, the obtained preintercalated materials are slightly different. Chemical preintercalation is easy to implement for large-scale lattice reconstruction but usually lacks precise control of the quantity of preintercalation, while electrochemical methods usually provide the opposite traits due to the precise control of voltage and reaction time.

To clarify the functionality of preintercalation, a series of concrete examples are given below. Layered vanadium oxides with high capacity have been explored as the electrode in lithium-ion batteries (LIBs) for many years. However, poor rate performance and rapid capacity fading are still obstacles due to low electronic conductivity and poor structural stability of monoclinic vanadium oxides ( $\alpha$ - $V_2O_5$ ). Hence, in order to overcome the above obstacles, a chemical preintercalation approach has been utilized, with the complete phase transition from  $\alpha$ - $V_2O_5$  to alkali metal ion preintercalated  $\beta$ - $V_6O_{15}$ .<sup>12</sup> The capacity retention after 100 cycles was increased from 37.6% to over 95%. The rate capability of the preintercalated electrodes was also much higher than that of the pristine  $\alpha$ - $V_2O_5$ . Beyond that, the preintercalated  $\delta$ - $M_xV_2O_5$  ( $M = Li, Na, K, Mg, \text{ and } Ca$ ) was systematically constructed from bilayer vanadium oxides by Pomerantseva et al.<sup>13</sup> The performances of these electrodes show an experimental rule that rate capability and cyclability improve with increasing hydrated ion radius of preintercalation ions. Furthermore, a great deal of preintercalated electrodes, such as  $V_2O_5$ ,<sup>14–18</sup>  $V_6O_{13}$ ,<sup>19</sup>  $MoO_3$ ,<sup>20,21</sup>  $MoS_2$ ,<sup>22,23</sup>  $MnO_2$ ,<sup>24–28</sup>  $Fe_2(MoO_4)_3$ ,<sup>29</sup>  $VOPO_4$ ,<sup>30,31</sup>  $(Ni_xMn_yCo_z)O_2$ ,<sup>32,33</sup> and carbon-based materials,<sup>34–36</sup> with improved performances for batteries and supercapacitors have been reported over the past few years.

In the previous section, we stated that some preintercalation electrodes do reveal better performance, including high reversible capacity, outstanding rate capability, and extended

cycles. Unfortunately, despite several previous great investigations, the overall mechanisms explaining how preintercalation improves battery performance are still ambiguous. In this Perspective, we compare the electrochemical performance of preintercalated electrodes vs the corresponding pristine electrodes, reveal the relationships between diverse preintercalation ions and electrochemical properties, and conclude most of the fundamental mechanisms of preintercalation efforts. The detailed illustrations, sorted by functions, are shown below.

**Electronic Conductivity.** It is no doubt that electrical conductivity is one of the most crucial factors in electrochemical reactions. The insufficient conductivity of electrodes results in strong polarization, leading to negative impacts on both capacity and rate capability. Theoretically, the majority of insertion-type cathodes are semiconductors, and the minority are insulators, which are composed of almost or fully empty conduction bands and almost or fully occupied valence bands, respectively. In band theory (Figure 2a), there is an energy gap ( $E_G$ ) to separate the

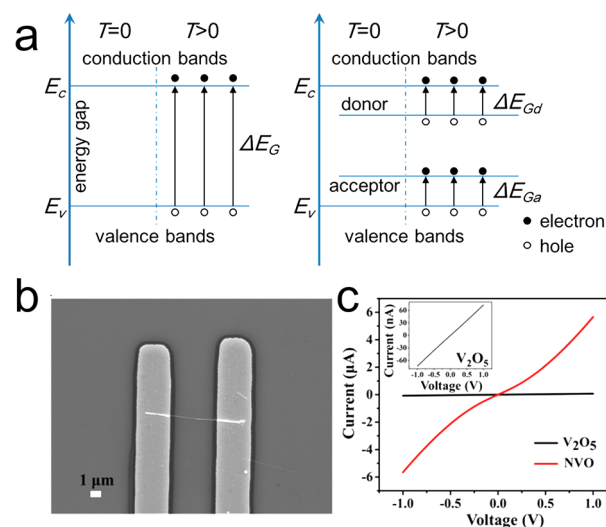


**Figure 2.** (a) Energy band diagrams of electrode materials before (left figure) and after (right figure) doping or preintercalation. (b) Scanning electron microscopy image of the single  $\delta$ - $Na_{0.33}V_2O_5$  nanowire device. (c)  $I$ - $V$  curves of the pristine  $\alpha$ - $V_2O_5$  and preintercalated  $\delta$ - $Na_{0.33}V_2O_5$  (NVO). Reprinted with permission from ref 38. Copyright 2018 Wiley.

lowest-energy level of the conduction bands ( $E_C$ ) from the topmost energy level of the valence bands ( $E_V$ ). At a certain temperature, the conductivity ( $\sigma$ ) is mainly determined by the density of the carrier (electrons and holes) and transport properties ( $\mu$  represents the migration rate of positive and negative charges; eq 1).

$$\sigma = nq\mu_- + pq\mu_+ \quad (1)$$

In many early studies, doping was considered a universal approach for improving electronic conductivity by introducing impurity levels within the energy gap, associated with increasing carrier density and modification of transport properties (Figure 2a). As for the electrode materials with cations ( $Li^+$ ,  $Na^+$ ,  $K^+$ ,  $Zn^{2+}$ ,  $Ca^{2+}$ , etc.) preintercalation, guest ions introduce shallow donor levels below the bottom of the conduction band and the electrons are easily donated from the donor level to the conduction band. On the other hand, as for the anion preintercalated materials, the negative ions introduce acceptor levels that could acquire the electrons from the valence band,

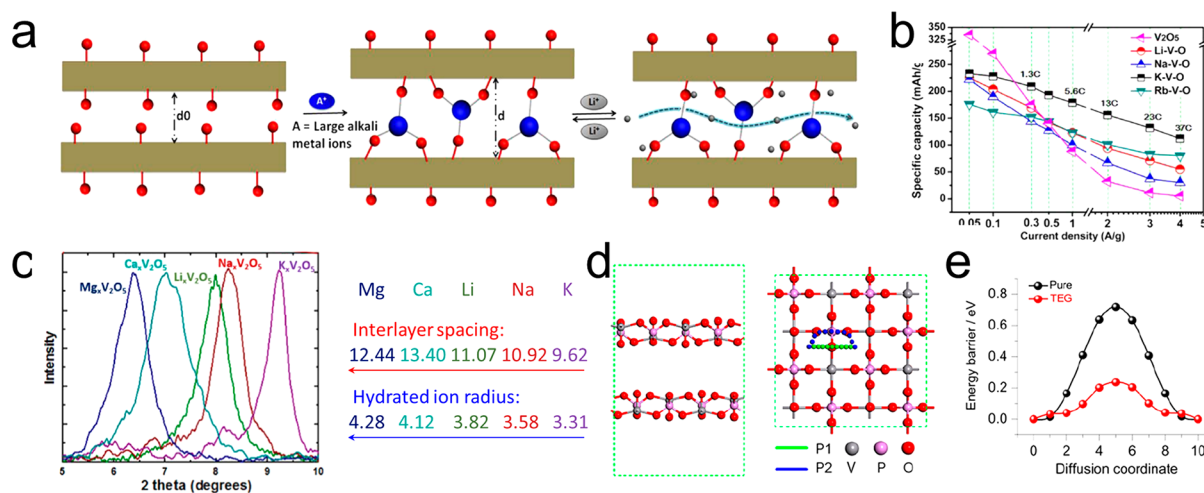


**Figure 3.** (a) Schematic illustration of large alkali metal ion preintercalation and an enlarged diffusion channel. (b) Rate performance of pristine  $\alpha$ -V<sub>2</sub>O<sub>5</sub> and preintercalated electrodes at various current rates from 0.05 to 4.0 A g<sup>-1</sup>. Reprinted with permission from ref 12. Copyright 2015 American Chemical Society. (c) X-ray diffraction (XRD) patterns of V<sub>2</sub>O<sub>5</sub> with different ions preintercalation in the position of the (001) peak (left) and the correlation between interlayer spacings and hydrated ion radii with units of Å (right). Reprinted with permission from ref 13. Copyright 2018 Elsevier. (d) Geometric structures of  $\alpha$ 1-VOPO<sub>4</sub> and possible ion diffusion pathways. (e) Diffusion barrier (minimum-energy path) profiles of sodium ion transport in initial  $\alpha$ 1-VOPO<sub>4</sub> (pure) and the triethylene glycol (TEG) preintercalated VOPO<sub>4</sub>. Reprinted with permission from ref 31. Copyright 2017 American Chemical Society.

leading to “hole” formation in the valence band. Nevertheless, in most electrode materials, because of the terminal negative oxygen and sulfur that strongly repel the negative charge, it is difficult to preintercalate anions into the interlayer spacing of the host.

In order to understand the electrical transport property of the preintercalated electrode experimentally, a solid-state single molybdenum oxide nanobelt test platform was employed by Mai and co-workers in 2007, in which it can avoid effects of binders and conductive additives during the battery assembling process.<sup>20</sup> The corresponding results suggested that the MoO<sub>3</sub> electrodes are converted from semiconductor ( $\sim 10^{-4}$  S m<sup>-1</sup>) to metallic behavior ( $10^{-2}$  S m<sup>-1</sup>) after chemical preintercalation of Li<sup>+</sup> ions.<sup>20</sup> Furthermore, a recent paper has proved that intercalating organic viologen cations into the interlayer region also enhances the conductance of MoO<sub>3</sub>.<sup>37</sup> He et al. developed a Na<sup>+</sup> ions preintercalated vanadium oxide cathode ( $\delta$ -Na<sub>0.33</sub>V<sub>2</sub>O<sub>5</sub>) by chemical preintercalation process. The electrical conductivities of the pristine nanowire and Na<sup>+</sup> ion preintercalated nanowire were tested through a single-nanowire test platform (Figure 2b), and results show that the conductivity is greatly improved from 7.3 S m<sup>-1</sup> (pristine  $\alpha$ -V<sub>2</sub>O<sub>5</sub>) to  $5.9 \times 10^4$  S m<sup>-1</sup> ( $\delta$ -Na<sub>0.33</sub>V<sub>2</sub>O<sub>5</sub>) after the Na<sup>+</sup> ion preintercalation (Figure 2c).<sup>38</sup>

Combining the theoretical hypothesis and the experimental verifications, we can confirm that the preintercalation approach has great potential in improving the electronic conductivity of electrode materials, especially for materials with poor conductivity that seriously suppresses the electrochemical performance. On the other hand, in the preparation of electrodes, the integrated conductivity of electrodes is improved by mixing the conductive additives, such as acetylene black, ketjen black, and super P. However, a certain segment of the conductive additives leads to the descent of the mass-specific capacity of electrodes. Thus, the ascent of the electronic conductivity originating from preintercalation treatment not only makes for enhanced electrochemical performances but also would improve the

specific capacity of electrodes by reducing or exempting the usage of conductive additives.

**Ionic Diffusion Coefficient.** The ionic diffusion coefficient is another key factor in rechargeable batteries. Ceder et al. systematically studied the Li mobility factors in layered lithium transition metal oxides by using first-principles calculations and concluded that the Li slab spacing and the electrostatic repulsion were two dominant effects.<sup>39</sup> To some extent, interlayer spacing is affected by electrostatic interactions; that is, these above two effects are coupled. According to Coulomb’s law, the electrostatic interactions ( $u$ ) yield the following eq 2

$$u = \frac{k_e q_1 q_2}{r^2} \quad (2)$$

where  $k_e$  is Coulomb’s constant ( $k_e \approx 9.0 \times 10^9$  N m<sup>2</sup> C<sup>-2</sup>),  $q$  is the quantity of charge, and  $r$  represents the distance between charges. As the interlayer space becomes expanded in the  $c$  direction, the electrostatic interactions ( $u$ ) will diminish with the increase of the scalar ( $r$ ), and then the carrier ions will migrate farther away. Expanding interlayer spacing can relieve the electrostatic repulsion (diffusion barrier) between two of the guests (nonbonding interaction) or between guests and hosts (bonding interaction). The diminution of the migration barrier of carrier ions is reflected in the ionic diffusion coefficient, which can be experimentally measured through multiple-rate cyclic voltammetry, galvanostatic intermittent titration techniques, or electrochemical impedance spectroscopy.

Zhao et al. quantitatively described the enhanced ionic diffusion by studying the chemical preintercalation of alkali metal ions into five typical cathode materials A–M–O ( $A = \text{Li, Na, K, Rb; } M = \text{V, Mo, Co, Mn, Fe–P}$ ).<sup>12</sup> Figure 3a shows the schematic illustration of large alkali metal ion preintercalation and an enlarged diffusion channel for lithium-ion diffusion. The structural models of the preintercalated compounds were obtained through rotation electron diffraction and X-ray diffraction measurements. The diffusion channel sizes were then estimated by using density functional theory based on the above models. It is noticeable that almost all of the

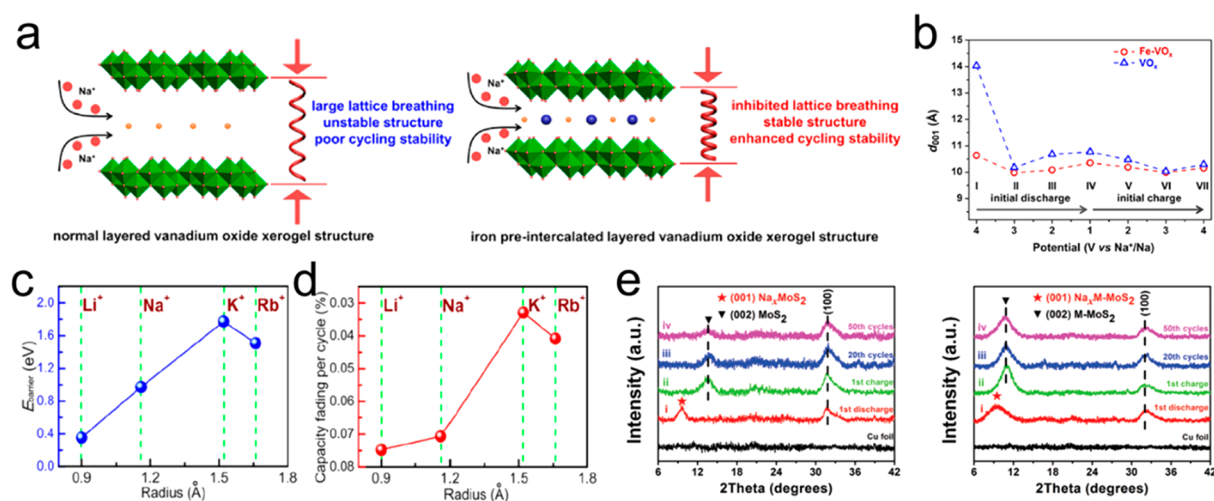


**Figure 4.** (a) Schematic illustration of the layered vanadium oxide xerogel with large lattice breathing and the iron preintercalated vanadium oxide xerogel with inhibited lattice breathing. (b) Lattice parameter ( $d_{001}$ ) difference between pristine and preintercalated vanadium oxide during the first discharge-charge process. Reprinted with permission from ref 15. Copyright 2015 American Chemical Society. (c) Diffusion barrier ( $E_{\text{barrier}}$ ) of A ions ( $A = \text{Li}^+, \text{Na}^+, \text{K}^+, \text{Rb}^+$ ) in A-V-O obtained from ab initio calculations. (d) Capacity fading per cycle vs the radius of different preintercalation ions at a current density of  $1.0 \text{ A g}^{-1}$ . Reprinted with permission from ref 12. Copyright 2015 American Chemical Society. (e) Ex situ XRD patterns of pristine  $\text{MoS}_2$  and methyl-functionalized M- $\text{MoS}_2$  during cycling at a current density of  $1.0 \text{ A g}^{-1}$ : (i) first discharge to 0.6 V, (ii) first charge to 3 V, (iii) after 20 cycles, and (iv) after 50 cycles. Reprinted with permission from ref 22. Copyright 2017 Royal Society of Chemistry.

preintercalated vanadium oxide electrodes with enlarged channel sizes show a better rate performance than the pristine  $\alpha\text{-V}_2\text{O}_5$  electrode. Remarkably, the K-V-O electrode, which has the largest interlayer spacing, exhibits the highest rate capability, indicating that the enlarged diffusion channel can facilitate Li migration in the interlayer region during the charge-discharge process (Figure 3b). As another example of preintercalated vanadium oxides,  $\delta\text{-K}_x\text{V}_2\text{O}_5 \cdot n\text{H}_2\text{O}$  has been successfully demonstrated as a record-high-capacity cathode material ( $268 \text{ mAh g}^{-1}$ ) for potassium-ion batteries by Pomerantseva et al.<sup>9</sup> With the help of  $\text{K}^+$  ion preintercalation during the chemical process, the interlayer spacing has been expanded to up to 9.65 Å, which greatly contributes to the facilitated diffusion of  $\text{K}^+$  ion carriers. This phenomenon has also been observed in layered iron/manganese-based oxides for sodium-ion batteries in the previous work of Wang et al.<sup>40</sup> On account of the expanded interlayer structure originating from large-sized  $\text{K}^+$  ion preintercalation through a chemical procedure, the diffusion coefficient of  $\text{Na}^+$  ion carriers has been greatly increased and the as-prepared electrode ( $\text{K}_{0.7}\text{Fe}_{0.5}\text{Mn}_{0.5}\text{O}_2$ ) shows the highest reversible capacity at various current densities for sodium-ion batteries, compared with  $\text{Li}^+$  and  $\text{Na}^+$  ion preintercalated electrodes. Insertion of alkali metal ions and bivalent alkaline earth metal ions into bilayered vanadium oxide has been systematically investigated by Pomerantseva et al., and their results show that the interlayer distance of  $\delta\text{-M}_x\text{V}_2\text{O}_5$  ( $M = \text{Li}, \text{Na}, \text{K}, \text{Mg}, \text{and Ca}$ ) increases with the increase of the hydrated radius of preintercalation ions (Figure 3c).<sup>13</sup>

Expanded interlayer spacing is not only driven from the preintercalation of alkali metal ions or alkaline earth metal ions, but it is also achievable by preintercalation of water, organic molecules, or co-intercalation of ions and water. For instance, bilayered vanadium oxides xerogel with water preintercalation ( $\text{V}_2\text{O}_5 \cdot n\text{H}_2\text{O}$ ) by chemical process has been studied as the cathode material for Mg and Zn batteries.<sup>16,41</sup> Its crystallographic structure could be described as pairs of single

monoclinic  $\text{V}_2\text{O}_5$  layers separated by water molecules and stacked along the  $z$ -axis, which was determined through the atomic pair distribution function technique by Petkov et al. for the first time.<sup>42</sup> Because of the large interlayer spacing for facile ion (de)insertion,  $\text{V}_2\text{O}_5 \cdot n\text{H}_2\text{O}$  exhibits improved performance compared with traditional  $\alpha\text{-V}_2\text{O}_5$ . Layered polyanion-type  $\alpha\text{-VOPO}_4$  with organic molecule (triethylene glycol or tetrahydrofuran) preintercalation was developed through a chemical displacement reaction by Peng and co-workers in 2017.<sup>31</sup> X-ray absorption fine structure characterization revealed that the selectable organic guests are successfully intercalated into the individual  $\text{VOPO}_4$ , leading to a controllably expanded interlayer spacing. The improved  $\text{Na}^+$  ion transport kinetics, reflected in enhanced rate performance of sodium-ion batteries, has been supported by the small calculated energy barrier (Figure 3d,e). Another example of  $\text{VOPO}_4$  with ultralarge expanded structure ( $d$ -spacing of 1.4 nm) has been introduced for magnesium batteries by the same displacement reaction with phenylamine molecules.<sup>30</sup> Such a large expanded interlayer spacing is attributed to the stacking of bilayer phenylamine molecules onto the layered structure of the  $\text{VOPO}_4$  host, substantially relieving the diffusion kinetics issues in the multivalent  $\text{Mg}^{2+}$  ion battery.

In this section, the dominant mechanism of diffusion improvement in preintercalated electrodes has been attributed to the diminution of electrostatic interactions because of the preintercalation-induced interlayer spacing expansion. In particular, this improvement is more obvious in the electrodes with preintercalation of large radius or hydrated radius ions. A series of previous experimental proofs have indicated that the preintercalation approach could effectively be conducive to improving the migration of ion carriers in the electrode materials which suffer from the low ionic diffusion coefficient. It is also worth noting that excessive intercalation could lead to the split of host material especially for the two-dimensional layered electrode materials into single layer structures or collapse following the loss of electrochemical activity. Thus, the

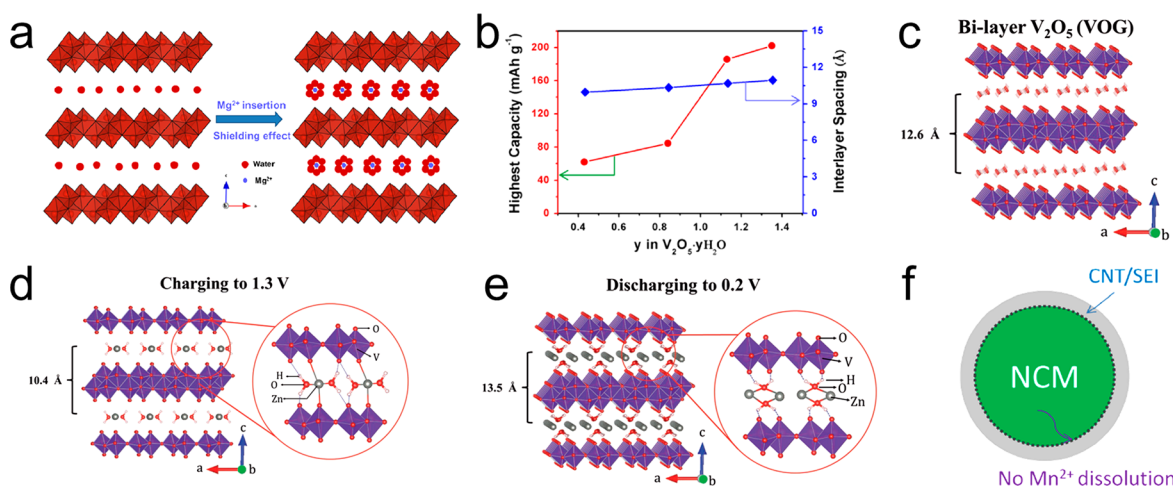


**Figure 5.** (a) Schematic illustration of the screening effect and (b) effect of crystal water content on the capacity and interlayer spacing in  $V_2O_5 \cdot nH_2O$  for the Mg battery. Reprinted with permission from ref 17. Copyright 2015 Elsevier. (c) Proposed crystal structures of  $V_2O_5 \cdot nH_2O$ , (d) after charging to 1.3 V and (e) discharging to 0.2 V for aqueous Zn-ion batteries. Reprinted with permission from ref 16. Copyright 2018 Wiley. (f) Mechanism of the electrolyte interphase engineered by the prelithiation protocol to prevent Mn(II) dissolution in  $Li(Ni_xMn_yCo_z)O_2$  material. Reprinted with permission from ref 33. Copyright 2015 American Chemical Society.

optimized species and amount of preintercalation for specific electrode material/crystal structure still need to be systemically investigated.

**Inhibiting “Lattice Breathing”.** During the charge–discharge process, ions are extracted from (or inserted into) the electrode structure, and in most cases, this leads to the changes in internal strain and stress. O3-type layered cathode materials, for example, are used to illustrate the above phenomenon.<sup>43</sup> There is an increased lattice parameter  $c$  of the unit cell owing to the intensive repulsion force between the two neighboring oxygen layers caused by Li extraction (charge). The upward oxidation states of the center metal contribute to shrinking of metal–oxygen bonds at the same time, leading to a decrease of parameters  $a$  and  $b$ . The changes in parameters reverse directions during Li insertion (discharge). These types of expansion and shrinkage during the electrochemical reactions are called “lattice breathing”.<sup>43</sup> It is no doubt that this repeated “breathing” leads to irreversible damage of the lattice structure, especially in the  $c$  direction. Over time, collapse of the structure occurs, leading to severe capacity fading. Furthermore, other layered types of electrode structures, such as  $V_2O_5$ ,  $LiVO_2$ ,  $LiNbO_2$ ,  $MoS_2$ , and so forth,<sup>43</sup> have also been observed to have this phenomenon (some materials show an opposite tendency of expansion and contraction during (de)insertion, which depends on which interaction is dominant).

To suppress this collapse, some pillar ions in the interlayer region have been introduced to stabilize the layered structure. Wei et al. developed a vanadium oxide xerogel with  $Fe^{3+}$  ion preintercalation ( $Fe-VO_x$ ) for sodium-ion batteries.<sup>15</sup> Because of the prestricted interlayer spacing originating from the strong electrostatic attraction between positive iron atoms and terminal negative oxygen atoms, the lattice breathing is well inhibited during the (de)sodiation process, which is conducive to enhancing the cycling stability (Figure 4a,b). To reveal the deep-layer theoretical illustration of relationships between the preintercalated vanadium oxide containing different preintercalation ions and corresponding cycling stabilities of lithium-ion storage, Zhao et al.<sup>12</sup> combined the theoretical calculated diffusion behaviors (diffusion barrier,  $E_{\text{barrier}}$ ) of preintercalation ions in hosts and the experimental atomic absorption spectroscopy

results, which reflect the deintercalation amounts of preintercalation ions from hosts (Figure 4c,d). They found that the larger diffusion barrier of preintercalation ions is, the less they are deintercalated from the hosts and the better the cycling properties of the preintercalated vanadium oxide materials are. Then they concluded that appropriate large alkali metal ion intercalation in the admissible crystal structure (without structure damage) can stabilize the diffusion channel, leading to enhanced cycling stability. In addition, when comparing the sodium-ion storage performances of pristine  $MoS_2$  to that of methyl-functionalized  $MoS_2$ , Huang et al. found that methyl-functionalized samples exhibit much better cycling stability.<sup>22</sup> The ex situ XRD results indicate that the interlayer change of pristine  $MoS_2$  is up to 42% and that of the methyl-functionalized sample is only 16%, which demonstrates that organic molecules and functional groups also play important roles as the pillars in inhibiting lattice breathing (Figure 4e). For the aqueous Zn-ion battery, Nazar et al.<sup>14</sup> first found that water spontaneously intercalated into the structure of  $\sigma-Zn_{0.25}V_2O_5$  when the electrode was immersed into an aqueous electrolyte and deintercalated accompanying  $Zn^{2+}$  intercalation upon electrochemical discharge. The (de)intercalation of water can buffer the electrode lattice parameter change, especially in the high-capacity electrode for multivalent ions storage.

In terms of the electrode materials with lattice breathing-induced poor cycling stability, the inhibiting effect is one of the best ways to tackle this insufficient cycling, and it could be easily achievable through preintercalation. However, it should be noticed that the interlayer spacing might shrink during preintercalation of positive ions (especially multiply charged ions), although it might be enlarged sometimes (depending on which interaction is dominant). The shrinkage of interlayer spacing probably gives rise to diminution of the ionic diffusion coefficient, which is detrimental to the rate performance of the electrode. Thus, while we try to improve the cycling stability by using the method of inhibiting “lattice breathing”, the side effects of multiply positive-charged ions cannot be underestimated.

**Screening Effect of Water Intercalation.** Generally, the stronger polarizing nature of multivalent ions compared with that of monovalent ions, which leads to the suppressive intercalation

kinetics, is one of the most fatal obstacles that cannot be ignored in the development of multivalent ion batteries, such as the ones utilizing  $\text{Mg}^{2+}$ ,  $\text{Ca}^{2+}$ ,  $\text{Zn}^{2+}$ , and  $\text{Al}^{3+}$  ions as charge carriers. Many researchers found that the multivalent ion batteries work better with aqueous electrolytes than nonaqueous systems and water co-intercalation exists in aqueous systems. It is well-known that the electrostatic repulsion ( $f$ ) between the two adjacent multivalent ions yields the following eq 3

$$f \propto \frac{1}{\epsilon_r r^2} \quad (3)$$

where  $\epsilon_r$  is the permittivity and  $r$  is the distance between two adjacent multivalent ions. Notably, the permittivity of water is approximately 80 at room temperature, which is much larger than that of vacuum and most common solvents. Therefore, the co-intercalated or structural water in host electrodes paves the way for facile migration of multivalent ions because the water molecules coordinate to multivalent ions as charge screening media to reduce the Coulombic repulsion (“lubricating” effect). The enhanced insertion reaction of  $\text{Mg}^{2+}$  ions into hydrated vanadium bronzes was reported as early as 1992.<sup>44</sup> After that, hydrated vanadium oxides with different contents of crystal water were systematically investigated by An et al.<sup>17</sup> By combining the results of electrochemical performance and structural characteristics, they concluded that the major role of the preintercalation is the shielding effect, which is related to reducing the diffusion barrier in the  $\text{Mg}^{2+}$  ion insertion reaction, rather than increasing the interlayer spacing (Figure 5a,b).  $\text{V}_2\text{O}_5 \cdot n\text{H}_2\text{O}$  was also investigated for aqueous Zn-ion batteries. The solid-state magic-angle-spinning nuclear magnetic resonance (NMR) technique was employed to explore the effects of structural water during the charge–discharge process, whose results clearly prove that water is highly involved in the electrochemical reactions (Figure 5c,d,e).<sup>16</sup> Because of the decreased effective charge of  $\text{Zn}^{2+}$  by the screening effect of water media, the water molecule preintercalated electrode exhibits a high energy density of  $144 \text{ Wh kg}^{-1}$  at a power density of  $10^4 \text{ W kg}^{-1}$ . Furthermore, screening effects can also function in Zn/water or Ca/water co-intercalation electrodes, which was proved by both Nazar et al. and Alshareef et al. Their results show that the water could facilitate the electrochemical (de)intercalation of  $\text{Zn}^{2+}$  ions into the structure.<sup>14,45</sup>

Although the screening effect of water is extraordinarily beneficial to reducing the electrostatic repulsion between ion carriers, it still has an obvious shortcoming. The electrodes modified by the screening effect are more stable in aqueous battery systems than organic battery systems as the organic systems usually work at a higher voltage (4.2 V) compared with aqueous systems (1.25 V). The existence of a water molecule at high voltage could be a severe safety issue because release of gas relevant to the decomposition of water could occur. That means that we need to do more testing when adopting this approach, particularly long-term cycling testing.

**Compensating Capacity Loss.** In battery systems, one of the main reasons for capacity loss is the loss of ion carriers, which is mostly related to the formation of a solid–electrolyte interface or irreversible metal plating at the anode side during the first cycle. This phenomenon is common in full-cell systems, especially in carbon materials with large surface area. In 2003, researchers realized that the excessive  $\text{Li}^+$  ions in the interlayered lattice can compensate for the first cycle capacity loss caused by the adverse reactions.<sup>46,47</sup> With the aid of a certain amount of excessive ion carriers on the anode and/or cathode side, the

carrier loss during the first cycle was compensated for and the remaining amount of active carriers during subsequent charge/discharge cycling was increased, resulting in an increase of reversible capacity.<sup>48</sup> In addition, another main reason is the activity loss of materials caused by dissolution of the active elements. The traditional  $\text{Li}(\text{Ni}_x\text{Mn}_y\text{Co}_z)\text{O}_2$  material, for example, suffers from severe capacity decay owing to the dissolution of Mn(II). In 2015, the preformed controllable solid–electrolyte interface by electrolyte reduction on the surface of materials during the electrochemical prelithiation process at about 1.2 V was reported. It can effectively restrain sustained Mn(II) dissolution into electrolyte, leading to outstanding retention of capacity (Figure 5f).<sup>35</sup> The agglomeration of active material could also lead to activity loss, which usually happens in conversion-type anodes. With this in mind, Xu et al. demonstrated a  $\text{Ca}^{2+}$  ion preintercalated conversion-type anode ( $\text{CaV}_4\text{O}_9$ ) by using a chemical method for sodium-ion batteries, which provided a promising way to tackle the issue of agglomeration.<sup>49</sup> During the first cycle, the nonactive CaO nanograins were generated from  $\text{Ca}^{2+}$  ions and uniformly distributed. Then they acted as a spectator, producing a self-preserving effect in the following cycles, inhibiting the agglomeration, and leading to better reversibility of the active components.

In this section, the preintercalation approach, which refers to the addition of excessive ions to the battery systems before cycling, is considered as a highly promising strategy to compensate for the activity losses, which include loss of ion carriers, dissolution of the active elements, and agglomeration of active material. Furthermore, physically mixing the additives (a small amount of corresponding metal or metal oxide powder) inside of the electrode materials is equally valid, which is used in some industrial applications for the same reason for compensating losses.

**Summary and Outlook.** As a promising optimization strategy that has gradually become a research hotspot, preintercalation that emphasizes an issues-oriented solution can target and overcome multiple limitations in electrode materials, including lack of electronic conductivity and ionic diffusion, “lattice breathing”, and strong polarizing of multivalent ions. Rationally designed preintercalated electrodes have shown dramatic improvements in electrochemical properties, such as capacity, rate capability, and cycling stability, compared with corresponding nonintercalated electrodes. However, although prior research has identified many successful cases, challenges and opportunities still exist in application of the preintercalation strategy.

First, in some preintercalated electrodes, it is inevitable that the preintercalation guest species deintercalate from the host structure into the electrolyte during cycling. This process causes the following two issues: (1) The diffusion ions from the electrolyte occupy the sites previously taken by preintercalation species, causing degradation of electrodes and the loss of carriers in the electrolyte. This phenomenon severely removes the advantages of preintercalated electrodes. (2) The guest species, especially in the case of water molecules, can act as the catalyst and/or reactant, resulting in severe decomposition of the organic electrolyte and/or undesirable side reactions at the electrode sides. It not only causes degradation of battery performance but also may lead to safety problems because of the gas generation and thermal release accompanying this process. Therefore, more effort should be paid to clarify the optimum amount of preintercalation, which could avoid deintercalation of

preintercalation species. Besides, long-term testing and high/low-temperature testing are compulsory because this is related to safety concerns.

Despite the fact that prior research has confirmed many successful cases, challenges and opportunities for developing preintercalated electrodes still exist.

Second, although the preintercalated electrodes have better electrochemical performance, the additional cost of the preintercalation strategy must be taken into account. Actually, some preintercalation methods are too complex and expensive to be used in large-scale industrial production. For instance, it is unpractical to realize large-scale producing preintercalated electrodes by using electrochemical preintercalation methods with current conditions of industrial techniques. Thus, it is strongly recommended that the feasibility of preintercalation methods should be assessed based on the real conditions before developing preintercalated electrodes, and the investigation of emerging general preintercalation methods is very meaningful.

Undeniably, the preintercalation strategy is an especially useful and issues-oriented solution to provide fundamental optimizations and overcome many intrinsic limitations through intelligent design. A rich variety of preintercalation methods can be tuned and adapted to improve the performance of electrodes that have specific disadvantages. We believe that this Perspective will provide guidance and offer new ideas for electrode researchers in developing prominent next-generation batteries.

## AUTHOR INFORMATION

### Corresponding Authors

\*E-mail: [yunlong.zhao@surrey.ac.uk](mailto:yunlong.zhao@surrey.ac.uk)

\*E-mail: [mlq518@whut.edu.cn](mailto:mlq518@whut.edu.cn)

### ORCID

Yunlong Zhao: 0000-0002-7574-7315

Liqiang Mai: 0000-0003-4259-7725

### Notes

The authors declare no competing financial interest.

### Biographies

**Xuhui Yao** is a joint Ph.D. candidate at Wuhan University of Technology and the University of Surrey, working with Prof. Liqiang Mai and Dr. Yunlong Zhao. He is also a visiting student under the supervision of Prof. Fernando A. Castro at the National Physical Laboratory, U.K. His research focuses on electrode materials for sodium/potassium-ion batteries and in situ electrochemical probing.

**Yunlong Zhao** is Assistant Professor at the University of Surrey with joint appointment at the National Physical Laboratory, U.K. as Senior Research Scientist. He carried out his postdoctoral research under the advice of Prof. Charles Lieber at Harvard University in 2014–2018. His current research interests focus on novel energy storage devices and electrochemical probing, nanobioelectronic devices/sensors, and 3D soft electronic systems.

**Fernando A. Castro** is a Principal Research Scientist at the National Physical Laboratory, U.K. He is also a Visiting Professor at the University of Surrey and the chair of the technical working area TWA36 Printed, Flexible and Stretchable Electronics of VAMAS. His research interests focus on developing reliable methods to understand the relationship between structure and function in new electronic and energy materials.

**Liqiang Mai** is Chang Jiang Scholar Chair Professor of Materials Science and Engineering at Wuhan University of Technology (WUT). He received his Ph.D. from WUT in 2004 and carried out his postdoctoral research in Prof. Zhonglin Wang's group at Georgia Institute of Technology in 2006–2007. His current research interests focus on new nanomaterials for electrochemical energy storage and micro/nanoenergy devices.

## ACKNOWLEDGMENTS

This work was supported by the National Natural Science Fund for Distinguished Young Scholars (51425204), the National Natural Science Foundation of China (51832004 and 51521001), the Programme of Introducing Talents of Discipline to Universities (B17034), the Yellow Crane Talent (Science and Technology), the Advanced Technology Institute at University of Surrey, and the UK National Measurement System.

## REFERENCES

- (1) Huang, Y.; Zheng, Y.; Li, X.; Adams, F.; Luo, W.; Huang, Y.; Hu, L. Electrode Materials of Sodium-Ion Batteries toward Practical Application. *ACS Energy Lett.* **2018**, *3*, 1604–1612.
- (2) Meng, J.; Guo, H.; Niu, C.; Zhao, Y.; Xu, L.; Li, Q.; Mai, L. Advances in Structure and Property Optimizations of Battery Electrode Materials. *Joule* **2017**, *1*, 522–547.
- (3) Tarascon, J.-M.; Armand, M. Issues and Challenges Facing Rechargeable Lithium Batteries. *Nature* **2010**, *44*, 171–179.
- (4) Armand, M.; Tarascon, J.-M. Building Better Batteries. *Nature* **2008**, *451*, 652–657.
- (5) Huggins, R. *Advanced Batteries: Materials Science Aspects*; Springer Science & Business Media, 2008.
- (6) Mizushima, K.; Jones, P.; Wiseman, P.; Goodenough, J. B.  $\text{Li}_x\text{CoO}_2$  ( $0 < x < 1$ ): A New Cathode Material for Batteries of High Energy Density. *Mater. Res. Bull.* **1980**, *15*, 783–789.
- (7) Padhi, A. K.; Nanjundaswamy, K. S.; Goodenough, J. B. Phospho-Olivines as Positive-Electrode Materials for Rechargeable Lithium Batteries. *J. Electrochem. Soc.* **1997**, *144*, 1188–1194.
- (8) Goodenough, J. B. Rechargeable Batteries: Challenges Old and New. *J. Solid State Electrochem.* **2012**, *16*, 2019–2029.
- (9) Clites, M.; Hart, J. L.; Taheri, M. L.; Pomerantseva, E. Chemically Preintercalated Bilayered  $\text{K}_x\text{V}_2\text{O}_5 \cdot n\text{H}_2\text{O}$  Nanobelts as a High-Performing Cathode Material for K-Ion Batteries. *ACS Energy Lett.* **2018**, *3*, 562–567.
- (10) Mao, M.; Gao, T.; Hou, S.; Wang, C. A Critical Review of Cathodes for Rechargeable Mg Batteries. *Chem. Soc. Rev.* **2018**, *47*, 8804–8841.
- (11) Hwang, J. Y.; Myung, S. T.; Sun, Y. K. Recent Progress in Rechargeable Potassium Batteries. *Adv. Funct. Mater.* **2018**, *28*, 1802938.
- (12) Zhao, Y.; Han, C.; Yang, J.; Su, J.; Xu, X.; Li, S.; Xu, L.; Fang, R.; Jiang, H.; Zou, X.; Song, B.; Mai, L.; Zhang, Q. Stable Alkali Metal Ion Intercalation Compounds as Optimized Metal Oxide Nanowire Cathodes for Lithium Batteries. *Nano Lett.* **2015**, *15*, 2180–2185.
- (13) Clites, M.; Pomerantseva, E. Bilayered Vanadium Oxides by Chemical Pre-Intercalation of Alkali and Alkali-Earth Ions as Battery Electrodes. *Energy Storage Mater.* **2018**, *11*, 30–37.
- (14) Kundu, D.; Adams, B. D.; Duffort, V.; Vajargah, S. H.; Nazar, L. F. A High-Capacity and Long-Life Aqueous Rechargeable Zinc Battery Using a Metal Oxide Intercalation Cathode. *Nat. Energy* **2016**, *1*, 16119.
- (15) Wei, Q.; Jiang, Z.; Tan, S.; Li, Q.; Huang, L.; Yan, M.; Zhou, L.; An, Q.; Mai, L. Lattice Breathing Inhibited Layered Vanadium Oxide Ultrathin Nanobelts for Enhanced Sodium Storage. *ACS Appl. Mater. Interfaces* **2015**, *7*, 18211–18217.
- (16) Yan, M.; He, P.; Chen, Y.; Wang, S.; Wei, Q.; Zhao, K.; Xu, X.; An, Q.; Shuang, Y.; Shao, Y.; Mueller, K. T.; Mai, L.; Liu, J.; Yang, J. Water-Lubricated Intercalation in  $\text{V}_2\text{O}_5 \cdot n\text{H}_2\text{O}$  for High-Capacity and High-Rate Aqueous Rechargeable Zinc Batteries. *Adv. Mater.* **2018**, *30*, 1703725.

- (17) An, Q.; Li, Y.; Deog Yoo, H.; Chen, S.; Ru, Q.; Mai, L.; Yao, Y. Graphene Decorated Vanadium Oxide Nanowire Aerogel for Long-Cycle-Life Magnesium Battery Cathodes. *Nano Energy* **2015**, *18*, 265–272.
- (18) Clites, M.; Byles, B. W.; Pomerantseva, E. Effect of Aging and Hydrothermal Treatment on Electrochemical Performance of Chemically Pre-Intercalated Na–V–O Nanowires for Na-Ion Batteries. *J. Mater. Chem. A* **2016**, *4*, 7754–7761.
- (19) Tian, X.; Xu, X.; He, L.; Wei, Q.; Yan, M.; Xu, L.; Zhao, Y.; Yang, C.; Mai, L. Ultrathin Pre-Lithiated  $V_6O_{13}$  Nanosheet Cathodes with Enhanced Electrical Transport and Cyclability. *J. Power Sources* **2014**, *255*, 235–241.
- (20) Mai, L. Q.; Hu, B.; Chen, W.; Qi, Y. Y.; Lao, C. S.; Yang, R. S.; Dai, Y.; Wang, Z. L. Lithiated  $MoO_3$  Nanobelts with Greatly Improved Performance for Lithium Batteries. *Adv. Mater.* **2007**, *19*, 3712–3716.
- (21) Dong, Y.; Xu, X.; Li, S.; Han, C.; Zhao, K.; Zhang, L.; Niu, C.; Huang, Z.; Mai, L. Inhibiting Effect of  $Na^+$  Pre-Intercalation in  $MoO_3$  Nanobelts with Enhanced Electrochemical Performance. *Nano Energy* **2015**, *15*, 145–152.
- (22) Huang, L.; Wei, Q.; Xu, X.; Shi, C.; Liu, X.; Zhou, L.; Mai, L. Methyl-Functionalized  $MoS_2$  Nanosheets with Reduced Lattice Breathing for Enhanced Pseudocapacitive Sodium Storage. *Phys. Chem. Chem. Phys.* **2017**, *19*, 13696–13702.
- (23) Wang, Y.; Xing, G.; Han, Z. J.; Shi, Y.; Wong, J. I.; Huang, Z. X.; Ostrikov, K. K.; Yang, H. Y. Pre-Lithiation of Onion-Like carbon/ $MoS_2$  Nano-Urchin Anodes for High-Performance Rechargeable Lithium Ion Batteries. *Nanoscale* **2014**, *6*, 8884–8890.
- (24) Radhiyah, A. A.; Izan Izwan, M.; Baiju, V.; Kwok Feng, C.; Jamil, I.; Jose, R. Doubling of Electrochemical Parameters via the Pre-intercalation of  $Na^+$  in Layered  $MnO_2$  Nanoflakes Compared to  $\alpha$ - $MnO_2$  Nanorods. *RSC Adv.* **2015**, *5*, 9667–9673.
- (25) Jabeen, N.; Xia, Q.; Savilov, S. V.; Aldoshin, S. M.; Yu, Y.; Xia, H. Enhanced Pseudocapacitive Performance of  $\alpha$ - $MnO_2$  by Cation Preinsertion. *ACS Appl. Mater. Interfaces* **2016**, *8*, 33732–33740.
- (26) Cao, L. L.; Yu, B. Z.; Cheng, T.; Zheng, X. L.; Li, X. H.; Li, W. L.; Ren, Z. Y.; Fan, H. M. Optimized  $K^+$  Pre-Intercalation in Layered Manganese Dioxide Nanoflake Arrays with High Intercalation Pseudocapacitance. *Ceram. Int.* **2017**, *43*, 14897–14904.
- (27) Ye, Q.; Dong, R.; Xia, Z.; Chen, G.; Wang, H.; Tan, G.; Jiang, L.; Wang, F. Enhancement Effect of Na Ions on Capacitive Behavior of Amorphous  $MnO_2$ . *Electrochim. Acta* **2014**, *141*, 286–293.
- (28) Mai, L.; Li, H.; Zhao, Y.; Xu, L.; Xu, X.; Luo, Y.; Zhang, Z.; Ke, W.; Niu, C.; Zhang, Q. Fast Ionic Diffusion-Enabled Nanoflake Electrode by Spontaneous Electrochemical Pre-Intercalation for High-Performance Supercapacitor. *Sci. Rep.* **2013**, *3*, 1718.
- (29) Wang, N.; Yuan, H.; NuLi, Y.; Yang, J.; Wang, J. Pre-lithiation Activates  $Fe_2(MoO_4)_3$  Cathode for Rechargeable Hybrid  $Mg^{2+}/Li^+$  Batteries. *ACS Appl. Mater. Interfaces* **2017**, *9*, 38455–38466.
- (30) Zhou, L.; Liu, Q.; Zhang, Z.; Zhang, K.; Xiong, F.; Tan, S.; An, Q.; Kang, Y. M.; Zhou, Z.; Mai, L. Interlayer-Spacing-Regulated  $VOPO_4$  Nanosheets with Fast Kinetics for High-Capacity and Durable Rechargeable Magnesium Batteries. *Adv. Mater.* **2018**, *30*, 1801984.
- (31) Peng, L.; Zhu, Y.; Peng, X.; Fang, Z.; Chu, W.; Wang, Y.; Xie, Y.; Li, Y.; Cha, J. J.; Yu, G. Effective Interlayer Engineering of Two-Dimensional  $VOPO_4$  Nanosheets via Controlled Organic Intercalation for Improving Alkali Ion Storage. *Nano Lett.* **2017**, *17*, 6273–6279.
- (32) Wu, Z.; Ji, S.; Hu, Z.; Zheng, J.; Xiao, S.; Lin, Y.; Xu, K.; Amine, K.; Pan, F. Pre-Lithiation of  $Li(Ni_{1-x-y}Mn_xCo_y)O_2$  Materials Enabling Enhancement of Performance for Li-Ion Battery. *ACS Appl. Mater. Interfaces* **2016**, *8*, 15361–15368.
- (33) Wu, Z.; Ji, S.; Zheng, J.; Hu, Z.; Xiao, S.; Wei, Y.; Zhuo, Z.; Lin, Y.; Yang, W.; Xu, K.; Amine, K.; Pan, F. Pre-lithiation Activates  $Li(Ni_{0.5}Mn_{0.3}Co_{0.2})O_2$  for High Capacity and Excellent Cycling Stability. *Nano Lett.* **2015**, *15*, 5590–5596.
- (34) Zhang, J.; Liu, X.; Wang, J.; Shi, J.; Shi, Z. Different Types of Pre-Lithiated Hard Carbon as Negative Electrode Material for Lithium-Ion Capacitors. *Electrochim. Acta* **2016**, *187*, 134–142.
- (35) Ren, J.; Su, L.; Qin, X.; Yang, M.; Wei, J.; Zhou, Z.; Shen, P. Pre-lithiated Graphene Nanosheets as Negative Electrode Materials for Li-Ion Capacitors with High Power and Energy Density. *J. Power Sources* **2014**, *264*, 108–113.
- (36) Sivakkumar, S.; Pandolfo, A. Evaluation of Lithium-Ion Capacitors Assembled with Pre-Lithiated Graphite Anode and Activated Carbon Cathode. *Electrochim. Acta* **2012**, *65*, 280–287.
- (37) Wei, Y. Q.; Sun, C.; Chen, Q. S.; Wang, M. S.; Guo, G. C. Significant Enhancement of Conductance of a Hybrid Layered Molybdate Semiconductor by Light or Heat. *Chem. Commun.* **2018**, *54*, 14077.
- (38) He, P.; Zhang, G.; Liao, X.; Yan, M.; Xu, X.; An, Q.; Liu, J.; Mai, L. Sodium Ion Stabilized Vanadium Oxide Nanowire Cathode for High-Performance Zinc-Ion Batteries. *Adv. Energy Mater.* **2018**, *8*, 1702463.
- (39) Kang, K.; Ceder, G. Factors that affect Li Mobility in Layered Lithium Transition Metal Oxides. *Phys. Rev. B: Condens. Matter Mater. Phys.* **2006**, *74*, No. 094105.
- (40) Wang, X.; Hu, P.; Niu, C.; Meng, J.; Xu, X.; Wei, X.; Tang, C.; Luo, W.; Zhou, L.; An, Q.; Mai, L. New-type  $K_{0.7}Fe_{0.5}Mn_{0.5}O_2$  Cathode with an Expanded and Stabilized Interlayer Structure for High-Capacity Sodium-Ion Batteries. *Nano Energy* **2017**, *35*, 71–78.
- (41) Sa, N.; Kinnibrugh, T. L.; Wang, H.; Sai Gautam, G.; Chapman, K. W.; Vaughey, J. T.; Key, B.; Fister, T. T.; Freeland, J. W.; Proffitt, D. L.; et al. Structural Evolution of Reversible Mg Insertion into a Bilayer Structure of  $V_2O_5 \cdot nH_2O$  Xerogel Material. *Chem. Mater.* **2016**, *28*, 2962–2969.
- (42) Petkov, V.; Trikalitis, P. N.; Bozin, E. S.; Billinge, S. J.; Vogt, T.; Kanatzidis, M. G. Structure of  $V_2O_5 \cdot nH_2O$  Xerogel Solved by the Atomic Pair Distribution Function Technique. *J. Am. Chem. Soc.* **2002**, *124*, 10157–10162.
- (43) Zhou, Y.-N.; Ma, J.; Hu, E.; Yu, X.; Gu, L.; Nam, K.-W.; Chen, L.; Wang, Z.; Yang, X.-Q. Tuning Charge–Discharge Induced Unit Cell Breathing in Layer-Structured Cathode Materials for Lithium-Ion Batteries. *Nat. Commun.* **2014**, *5*, 5381.
- (44) Novák, P.; Scheifele, W.; Joho, F.; Haas, O. Electrochemical Insertion of Magnesium into Hydrated Vanadium Bronzes. *J. Electrochem. Soc.* **1995**, *142*, 2544–2550.
- (45) Xia, C.; Guo, J.; Li, P.; Zhang, X.; Alshareef, H. N. Highly Stable Aqueous Zinc-Ion Storage Using a Layered Calcium Vanadium Oxide Bronze Cathode. *Angew. Chem., Int. Ed.* **2018**, *57*, 3943–3948.
- (46) Johnson, C. S.; Kim, J.-S.; Kropf, A. J.; Kahaian, A. J.; Vaughey, J. T.; Fransson, L. M.; Edström, K.; Thackeray, M. M. Structural Characterization of Layered  $Li_xNi_{0.5}Mn_{0.5}O_2$  ( $0 < x \leq 2$ ) Oxide Electrodes for Li Batteries. *Chem. Mater.* **2003**, *15*, 2313–2322.
- (47) Aravindan, V.; Nan, S.; Keppeler, M.; Madhavi, S. Pre-lithiated  $Li_xMn_2O_4$ : A New Approach to Mitigate the Irreversible Capacity Loss in Negative Electrodes for Li-Ion Battery. *Electrochim. Acta* **2016**, *208*, 225–230.
- (48) Holtstiege, F.; Bärman, P.; Nölle, R.; Winter, M.; Placke, T. Pre-lithiation Strategies for Rechargeable Energy Storage Technologies: Concepts, Promises and Challenges. *Batteries* **2018**, *4*, 4.
- (49) Xu, X.; Niu, C.; Duan, M.; Wang, X.; Huang, L.; Wang, J.; Pu, L.; Ren, W.; Shi, C.; Meng, J.; et al. Alkaline Earth Metal Vanadates as Sodium-Ion Battery Anodes. *Nat. Commun.* **2017**, *8*, 460.